CARBON NANOTUBE COATED FABRIC-BASED THIN AND FLEXIBLE PRESSURE SENSORS WITH ULTRA-WIDE SENSING RANGE

Sagar M. Doshi[1,2], Amit Chaudhari[1,2], Colleen Murray[1,2], Jill Higginson[1], Erik T. Thostenson[1,2,3]

[1]Department of Mechanical Engineering, [2]Center for Composite Materials and
[3]Department of Materials Science and Engineering, University of Delaware
Newark, Delaware, USA

ABSTRACT

This research focuses on the development and validation of novel flexible piezoresistive sensors that can be integrated into functional fabrics and footwear. Formation of thin nanocomposite films of electrically conductive carbon nanotubes (CNTs) using a scalable electrophoretic deposition (EPD) technique enables the sensing functionality. Films in the range of 250 - 750 nm are created on a variety of natural (cotton, wool) and synthetic (aramid, spandex) fibers using the EPD process. In this research, non-woven aramid fabric with randomly oriented fibers are coated with carbon nanotubes and polyethyleneimine (PEI). The aramid fabric is placed in direct contact with an electrode and PEI functionalized CNTs deposited under a DC electric field. The nanocomposite film first forms on the backing electrode and continues to grow around the aramid fibers and uniformly coats fibers throughout the thickness of the fabric.

The pressure sensor exhibits a large change in the in-plane electrical conductivity when out-of-plane pressure is applied. Formation of additional fiber-fiber contacts as well as the creation of sponge-like piezoresistive nanocomposite interphase between the fibers likely causes the in-plane electrical conductivity changes. The piezoresistive pressure sensors have an ultra-wide range of pressure sensing, from the tactile range (< 10 kPa) to body weight range (~500 kPa) and very high pressures (40 MPa). This wide sensing range enables applications in broad fields such as e-skin for robotics, human-computer interaction, biomedical devices and gait analysis. The sensors are integrated into footwear and preliminary tests conducted to explore applications in gait analysis and validate the sensor response using a treadmill instrumented with force sensors.

1. INTRODUCTION

The development of flexible pressure sensors is of great interest in recent years for applications in the field of human motion analysis [1], soft robotics [2], human-machine interfacing [3], gesture recognition [4], and orthotics/prosthetics [5]. Space constraints and weight limitations make the use of many conventional pressure sensors difficult for these applications. Pressure sensors developed recently leverage piezoelectric and triboelectric sensing mechanisms. Sensors based on piezoresistive and capacitive mechanisms are also being studied extensively.

A wide range of conductive materials such ZnO nanowires [6], silver nanowires [7] silver nanoparticles [8], gold nanowires [9] and graphene [10] have been investigated to tailor and optimize the sensitivity and range of pressure measurement. Nanocarbon materials, such as

Copyright 2019. Used by the Society of the Advancement of Material and Process Engineering with permission.

SAMPE Conference Proceedings. Charlotte, NC, May 20-23, 2019. Society for the Advancement of Material and Process Engineering – North America.

graphene, carbon nanotubes and carbon nanofibers have also been examined for sensors due to their high electrical conductivity. Carbon nanotubes, in particular, are suitable candidates for creating flexible pressure sensors and electronics because of their mechanical flexibility, electrical conductivity and intrinsic carrier mobility. Nanotubes have been investigated for strain and damage sensing in composites as well as structural health monitoring of civil infrastructure [11-15], and they have been added to elastomers such as PDMS to create stretchable sensors [16]. An alternate approach to mixing carbon nanotubes in polymers is grafting them directly onto fibers or textiles. Carbon nanotubes have been grafted onto glass fibers for composites [17] and Doshi et al. [18] demonstrated the ability to graft nanotubes to synthetic polymer (aramid) and natural fibers (wool).

In this research, we discuss a scalable electrophoretic deposition (EPD) method of manufacturing carbon nanotube coated fabric-based flexible pressure sensors. A uniform coating of a nanocomposite comprising of polyethylenimine (PEI) functionalized carbon nanotube is deposited on the surface of aramid fibers which imparts the electrical conductivity and the piezoresistive sensing functionality to the fabric. These sensors have an extremely wide range of pressure sensing, from tactile pressures to body weight and even higher. Sensors are then integrated with footwear and investigated for potential applications in the analysis of human gait. The sensor response is validated using a treadmill instrumented with force sensors.

2. EXPERIMENTAL

2.1 Materials

An aqueous dispersion of 1 g/L of multi-walled carbon nanotubes (CM-95, Hanwha Nanotech) functionalized with PEI (Sigma-Aldrich) is created using an ultrasonicated-ozonolysis method [18, 19]. The pH of the dispersion is reduced using glacial acetic acid (Sigma Aldrich, USA) to 6 in order to protonate the amine groups and form a stable dispersion of positively charged carbon nanotubes. The surface charge on the nanotubes enables them to be deposited using an electric field using a process known as electrophoretic deposition (EPD), shown Figure 1(a). Figure 1(b) shows a schematic diagram of a carbon nanotube functionalized with PEI.

A non-woven aramid fabric (20601, 50 g/m^2, Technical Fiber Products) of randomly oriented fibers (Figure 1(c)) was used as the carrier fabric for the deposition of the PEI-CNT nanocomposite film. The non-conductive aramid fabric was placed on a stainless steel electrode and was held in direct contact with the help of elastic bands. A stainless steel counter electrode was positioned at a fixed distance parallel to the electrode with the aramid fabric. The electrode setup with the fabric is immersed in the aqueous dispersion of carbon nanotubes and electrophoretic deposition was carried out using a direct current field strength of 22 V/cm. Figure 1(d) shows a scanning electron micrograph of an aramid fiber cross-sectioned using a focused ion beam (FIB), revealing a uniform coating of the PEI-CNT nanocomposite film. The dimensions of the specimen were 100 x 25 mm laminated between 0.12 mm thick plastic sheets using a heat laminating machine (Figure 2(a)). To measure the electrical resistance, flash dry silver paint (04999-AB, Structure Probe, Inc., PA) was applied followed by attaching wires using conductive epoxy adhesive (40-3900, Epoxies etc, RI).

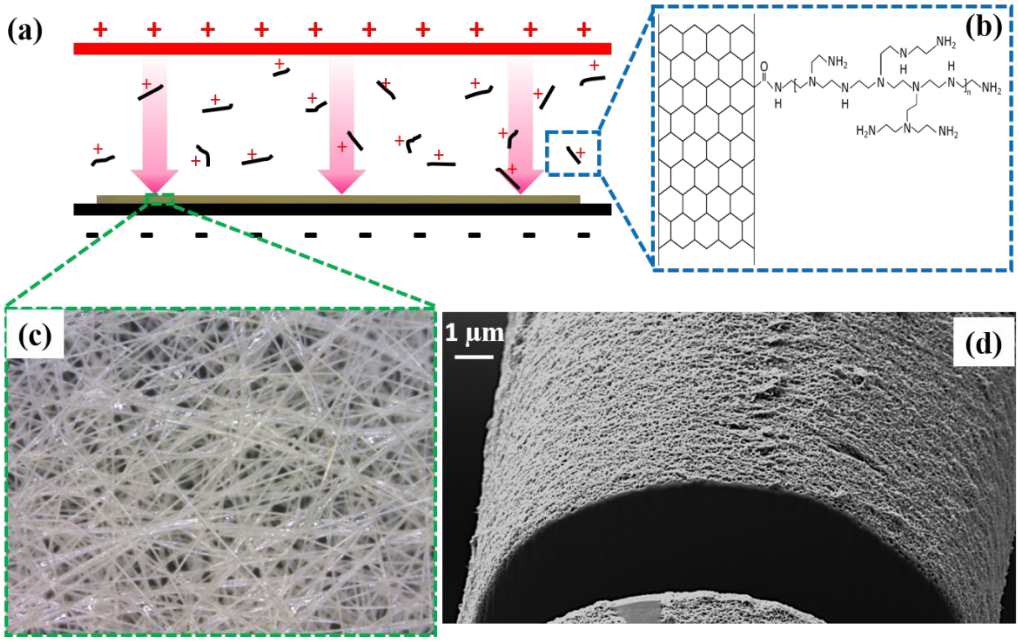


Figure 1: (a) A schematic diagram of the EPD process to deposit functionalized carbon nanotubes on non-woven aramid fabric. (b) An illustration of a carbon nanotube functionalized with polyethylenimine. (c) A picture of the non-woven aramid fabric taken using an optical microscope. (d) SEM micrograph of an aramid fiber cross-sectioned using Focused Ion Beam (FIB) showing a uniform coating of carbon nanotubes

2.2 Mechanical Characterization

The pressure was applied to the fabric sensor using an electrically actuated load frame (Instron 8562) with a 100 kN load cell (Figure 2(b)). The specimens were loaded to a pressure of 40 MPa followed by unloading. The electrical measurements for these experiments were performed using a Keithley 6430 sourcemeter. A constant voltage of 20V was applied while measuring the current to calculate the resistance. The load measurements were synchronized with electrical measurements using a customized LabVIEW interface.

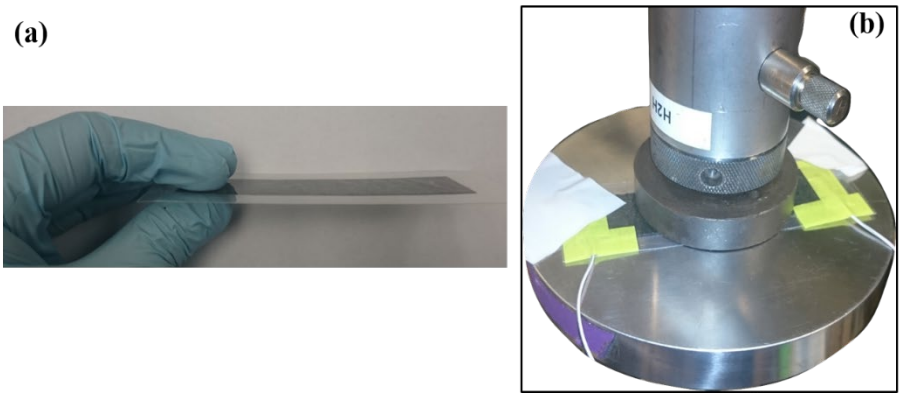


Figure 2: (a) An aramid fabric coated with carbon nanotubes laminated in plastic sheets. (b) Test setup for controlled pressure measurements.

2.3 Gait Analysis Tests on Treadmill with Force Sensors

To validate the sensor response for its application in gait analysis, sensors were integrated with footwear. Tests were conducted in the Neuromuscular Biomechanics Laboratory at the University of Delaware on an instrumented, split-belt treadmill (Bertec Corp., Worthington, OH). A single subject wearing the footwear integrated with the sensor walked at 0.75 m/s and 1.25 m/s for 1 minute. Treadmill force data was sampled at 2000 Hz and the sampling rate of the flexible pressure sensor was 30 Hz. The mass of the subject was 95 kilograms. Since the data acquisition system (DAQ) used in mechanical characterization was not portable, a smaller, easier to carry DAQ was built utilizing an Arduino Uno board powered by a 9V battery. A voltage dividing circuit is used for measurement of the resistance with a reference resistor of 10 kΩ. An additional 16 bit analog to digital converter is used to enhance the resolution of the measurement, and an SD card module stores the test data. The resistance change was normalized with respect to the baseline resistance of the sensor, i.e. when no load is applied.

In order to explore applications in detecting human motion, sensors were integrated into footwear and tests conducted on a treadmill instrumented with force sensors. The Aramid-CNT sensor was manufactured using the same processing conditions for the EPD process and attached in the hindfoot region of the footwear.

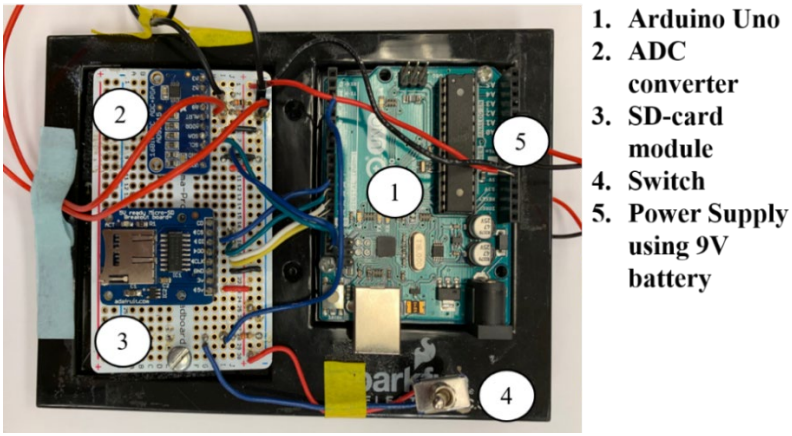


Figure 3: A photograph of the portable data acquisition system for measuring resistance during the gait analysis tests.

3. RESULTS

3.1 Sensor Response to Transverse Compressive Loads

The carbon nanotube coating on the aramid fibers imparts the sensing functionality to the fabric. An in-plane change in electrical resistance is observed on application of pressure because of the piezoresistive coating. Figure 4(a) shows the change in resistance due to the applied pressure for the Aramid-CNT specimen. The change in resistance is likely because of the formation of additional fiber-fiber electrical contacts under applied pressure and the local piezoresistive response due to the compression of the carbon nanotube coating – where the fiber-fiber contact resistance changes due to the local deformation of the carbon nanotube coating.

The slope of the resistance change at lower pressures is higher because the resistance change is dominated by the formation of fiber-fiber contacts. At higher pressures, the carbon nanotube coating is compressed on the surface of aramid fibers at the fiber-fiber contact points. Because of the piezoresistive nature of the carbon nanotube nanocomposite coating, the electrical resistance continues to decrease as the coating is compressed locally. Figure 4(b) is a micrograph of the specimen after compression, showing no significant damage to the aramid fibers. Figure 4(c) is an SEM micrograph showing localized deformation and flattening of the fibers at the fiber-fiber contact points. A slight decrease in the electrical resistance observed after the unloading of the sensors is possibly due to this local deformation of the fibers and increased fiber-fiber contact area.

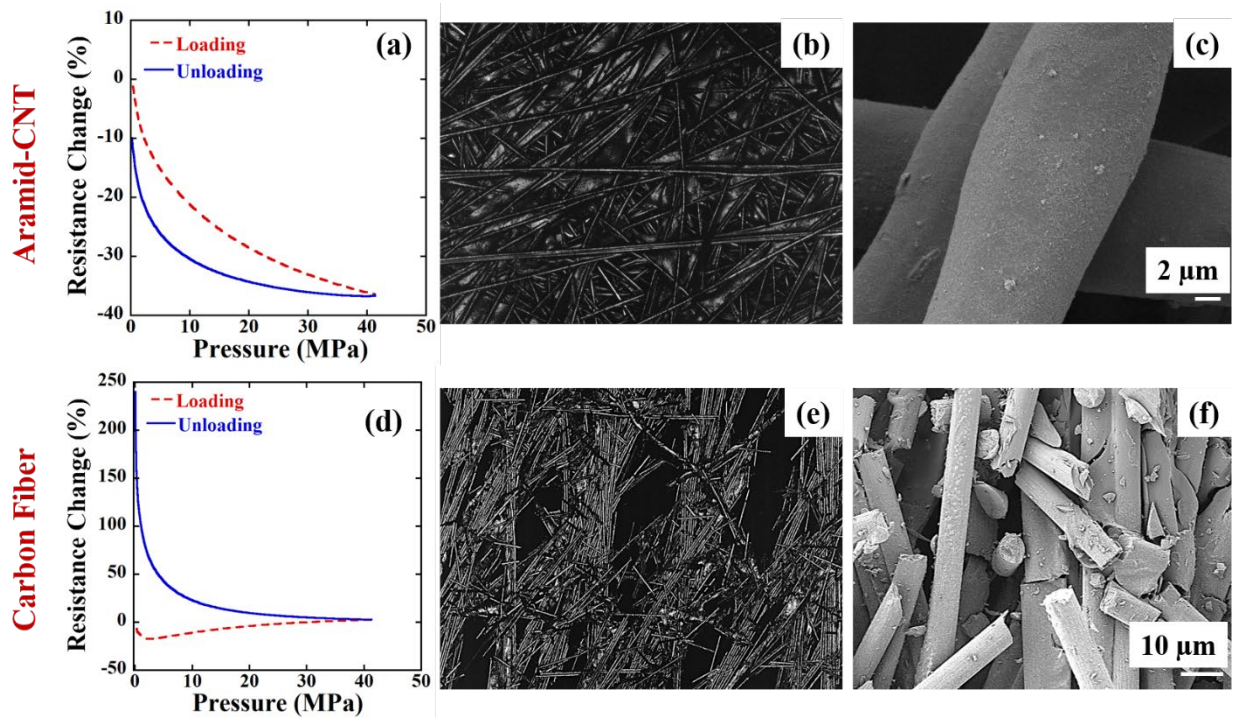


Figure 4: (a) Resistance response of Aramid-CNT specimen when loaded to 40 MPa followed by unloading. (b, c) Micrographs of the Aramid-CNT sensor after loading showing no significant damage. (d) Resistance response of the carbon fiber specimen. (e, f) Micrographs of carbon fiber specimen showing extensive damage.

A similar non-woven fabric (20301, 50g/m^2 Technical Fiber Products) of conductive carbon fibers was also subjected to the same pressure to further investigate the sensing mechanism. On application of pressure, the resistance decreases due to the formation of additional fiber-fiber contacts. However, unlike Aramid-CNT specimens, the electrical resistance of the loading curve shows a local minima at 2 MPa (Figure 4(d)). Upon further loading the sensor resistance increases and plateaus near 0% resistance change at pressures above 30 MPa. During the unloading phase, the resistance continues to increases continuously and a permanent resistance change of almost 250% is observed when completely unloaded. Figures 4(e) and 4(f) show the damage to the carbon fiber specimen after loading. The carbon fibers fracture on the application of the compression load, likely due to the bending at the fiber crossover points and the brittle nature of the fiber. For the Aramid-CNT specimen, no permanent change in resistance is observed when re-loaded below the

initial peak load of 40 MPa. Loading for the first time likely results in the localized fiber flattening observed at contact points (Figure 4(c)). After this initial localized deformation, the loading-unloading curves show a repeatable response.

3.2 Applications in Detecting Tactile Pressure and Human Gait Analysis

Figure 5 shows the sensing response when pressure is applied using a thumb. A resistance change of about 1.75% is observed under tactile pressure. When the pressure is applied, there is an immediate decrease in resistance without any noticeable delay. Upon removal of pressure, the resistance returns to its original value and no permanent change in resistance is observed. There is a slight overshoot upon unloading likely due to the lifting of the laminated sheet off of the fabric sensor. The sensor recovers almost immediately after removing the force.

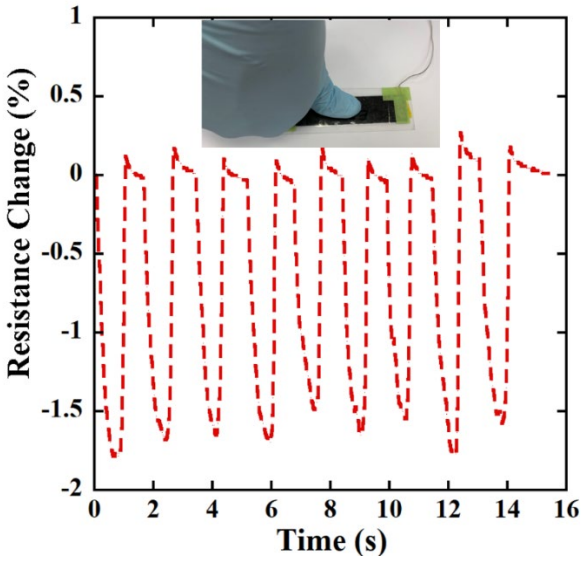


Figure 5: Sensing response of Aramid-CNT sensor when subjected to pressures applied by a thumb.

Figure 6(a) shows a photograph of the instrumented treadmill and 6(b) shows the sensor placed in the hindfoot region of a sandal.

Figure 6(c) shows a typical vertical ground reaction force (GRF) during walking. The GRF is represented as a percentage of body weight vs. gait cycle. This force curve is sometimes called the 'M curve' due to its shape. At the instant just before the heel strikes, the force is zero between the foot and ground. As the heel contacts the ground, the GRF will increase rapidly as the weight is transferred from the opposite limb. The GRF soon reaches 100% of the body weight. Because the body center of mass is still moving downwards and decelerating, the GRF increases beyond the body weight. The GRF reduces slightly below the full body weight due to the change in acceleration and the shift of weight from the hindfoot to the forefoot. Eventually, the GRF decreases to zero as body weight is shifted to the other limb and the foot lifted off the ground.

Walking at a faster speed generates a higher GRF. The average hindfoot peak GRF for each step is approximately 1000 N for 0.75 m/s and 1100 N for 1.25 m/s. Figures 7(a) and 7(b) shows the

absolute magnitude of the percentage resistance change measured from the sensor and force in Z direction measured from the instrumented treadmill for tests conducted at 0.75 m/s and 1.25 m/s, respectively. Since the sensor was covering only the hindfoot region, only a part of the 'M curve' is captured by the resistance sensor whereas the force plate captures the entire 'M curve.' The shape of the resistance curve closely resembles the GRF measured using the force plates as seen in Figures 7(a) and 7(b). The absolute magnitude of the percentage resistance change for 0.75 m/s is approximately 15% as compared to 18% for 1.25 m/s, shown in Figure 7(c).

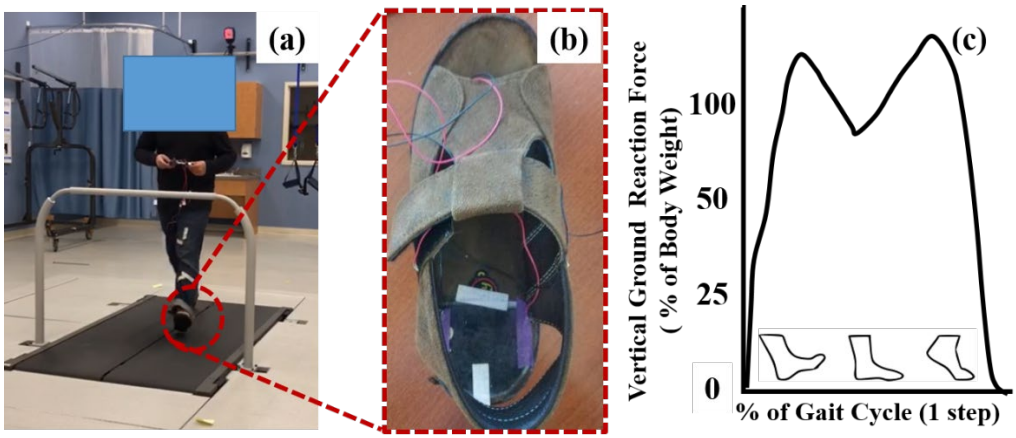


Figure 6: (a) Photograph of the treadmill instrumented with force sensors (b) Aramid-CNT sensor attached to the footwear. (c) Typical ground reaction force during a gait cycle

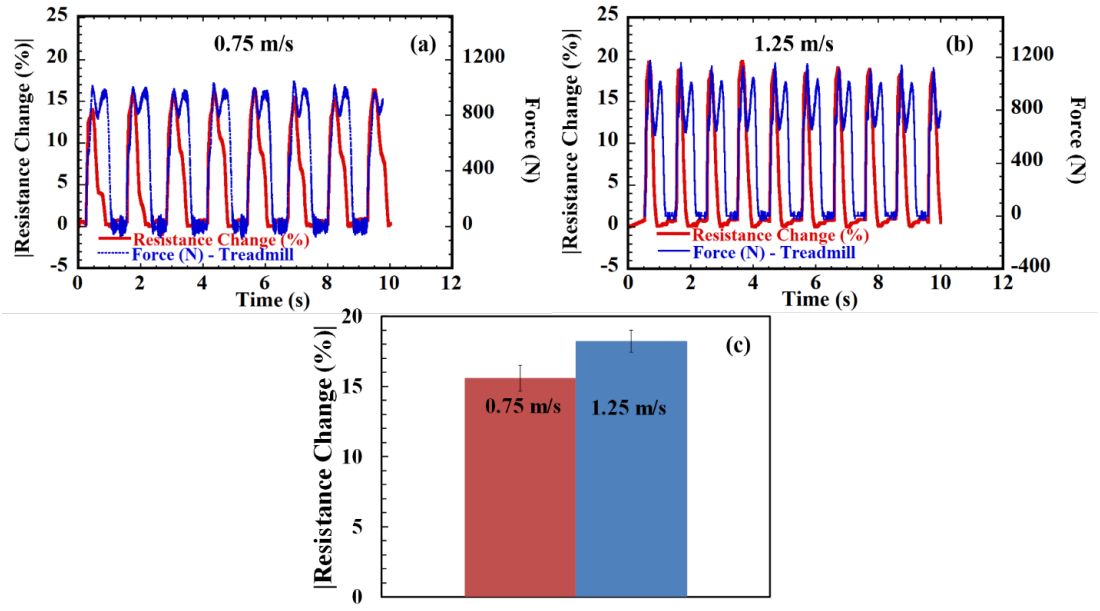


Figure 7: Absolute magnitude of percentage resistance change measured using Aramid-CNT sensors and the force in Z direction measured using instrumented treadmill for (a) 0.75 m/s and (b) 1.25 m/s. (c) Average value of peak resistance change for different walking speeds

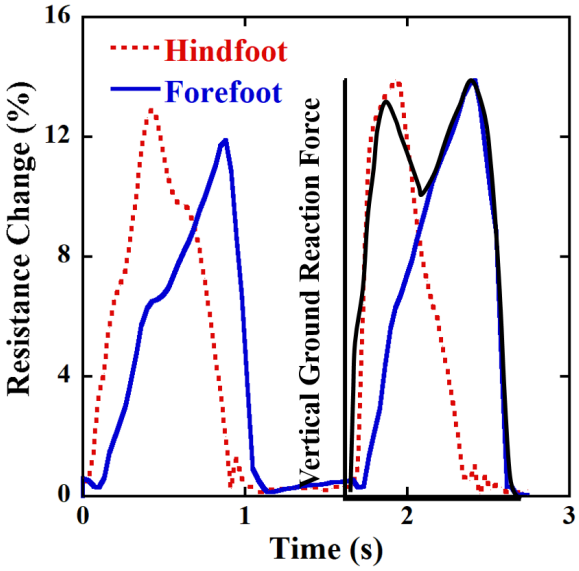


Figure 8: Resistance change for a pair of sensors attached in the footwear. The sensing response is similar to a typical ground reaction force.

To capture the entire 'M curve,' another sensor was attached in the forefoot. Figure 8 shows the absolute magnitude of the percentage resistance change of both sensors for 2 steps. In a particular gait cycle, when the heel touches the ground, the pressure is applied on the hindfoot sensor which causes a resistance change. As the weight is being transferred to midfoot, the magnitude of resistance change of hindfoot sensor decreases and the forefoot starts to increase. Just before 'push off', when all the body weight is near the toe of the foot, the forefoot sensor reaches its peak value before decreasing to zero when the foot is off the ground. One of the reasons why the percentage resistance change curve is slightly different from the GRF curve is due to incomplete coverage of the sensors by the foot. Drift in the sensor signal, calibration of resistance to force and testing on more subjects are some of the challenges that need to be addressed going forward.

Not only are the sensors able to detect different walking speeds, but they could also be potentially used for detecting gait imbalances in patients undergoing rehabilitation and track their improvement over time. Unlike the instrumented treadmill which gives an overall value of GRF, multiple sensors can be used to detect gait parameters such as heel strikes/toe strikes. The key advantages of using these sensors for gait analysis over an instrumented treadmill is the low cost and the ability to customize the footwear and sensor placement for every patient/athlete. More importantly, these sensors enable the gait measurement of subjects outside of the laboratory in their natural work or home environment. Measurements can be conducted over extended periods, unlike the instrumented treadmill where the clinician can monitor the subject for a limited amount of time.

4. CONCLUSIONS

A thin and flexible pressure sensor has been developed using a scalable and efficient electrophoretic deposition method to coat functionalized carbon nanotubes on a non-woven aramid

fabric. An extremely wide range of pressure detection capability was demonstrated – in the tactile range to body weight and even higher. Preliminary experiments are conducted for gait analysis using these sensors attached to footwear, and the sensing response is validated using an instrumented treadmill. The flexible sensor is able to measure some of the important gait characteristics such as speed of walking and heel strikes. This novel sensor has potential applications in the field of prosthetics, e-skins for robots, human-machine interaction and creation of smart garments used for human performance monitoring.

5. ACKNOWLEDGMENTS

Funding and support has been provided by the Delaware INBRE program, with a grant from the National Institute of General Medical Sciences – NIGMS (P20 GM103446), the state of Delaware, US National Science Foundation (Grant 1254540: Dr. Mary Toney, Program Director) and Unidel Foundation. The authors acknowledge Stephen Durabano and John Thiravong for helping in the mechanical characterization and Luke Nigro for assisting with the data collection on the instrumented treadmill. The authors thank National Institutes of Health NIH P30 GM 103333.

6. REFERENCES

1. Patel, Shyamal, et al. "A review of wearable sensors and systems with application in rehabilitation." *Journal of neuroengineering and rehabilitation* 9.1 (2012): 21. Trivedi, doi.org/10.1186/1743-0003-9-21
2. Trivedi, Deepak, et al. "Soft robotics: Biological inspiration, state of the art, and future research." *Applied bionics and biomechanics* 5.3 (2008): 99-117. dx.doi.org/10.1080/11762320802557865
3. Jung, Sungmook, et al. "Reverse-micelle-induced porous pressure-sensitive rubber for wearable human–machine interfaces. "*Advanced Materials* 26.28 (2014): 4825-4830. doi.org/10.1002/adma.201401364
4. Liang, Xiangpeng, Hadi Heidari, and Ravinder Dahiya. "Wearable Capacitive-Based Wrist-Worn Gesture Sensing System."*CAS (NGCAS), 2017 New Generation of*. IEEE, 2017. 10.1109/NGCAS.2017.80
5. Kim, Jaemin, et al. "Stretchable silicon nanoribbon electronics for skin prosthesis." *Nature communications* 5 (2014): 5747. 10.1038/ncomms6747 (2014)
6. Liao, Xinqin, et al. "A Highly Stretchable ZnO@ Fiber-Based Multifunctional Nanosensor for Strain/Temperature/UV Detection." *Advanced Functional Materials* 26.18 (2016): 3074-3081. doi.org/10.1002/adfm.201505223
7. Wang, Jun, et al. "A highly sensitive and flexible pressure sensor with electrodes and elastomeric interlayer containing silver nanowires." *Nanoscale* 7.7 (2015): 2926-2932. 10.1039/C4NR06494A
8. Lee, Jaehong, et al. "Conductive fiber-based ultrasensitive textile pressure sensor for wearable electronics." *Advanced materials* 27.15 (2015): 2433-2439. doi.org/10.1002/adma.201500009
9. Gong, Shu, et al. "A wearable and highly sensitive pressure sensor with ultrathin gold nanowires." *Nature communications*5 (2014): 3132. 10.1038/ncomms4132 (2014)

10. Tung, Tran Thanh, et al. "Recent advances in sensing applications of graphene assemblies and their composites." Advanced Functional Materials 27.46 (2017): 1702891. doi.org/10.1002/adfm.201702891

11. Thostenson, Erik T., and T-W. Chou. "Carbon nanotube networks: sensing of distributed strain and damage for life prediction and healing." *Advanced Materials* 18.21 (2006): 2837-2841. doi.org/10.1002/adma.200600977

12. Ahmed, Shafique, et al. "Integration of carbon nanotube sensing skins and carbon fiber composites for monitoring and structural repair of fatigue cracked metal structures." Composite Structures 203 (2018): 182-192. doi.org/10.1016/j.compstruct.2018.07.005

13. Ahmed, Shafique, et al. "Development of a novel integrated strengthening and sensing methodology for steel structures using CNT-based composites." *Journal of Structural Engineering* 143.4 (2016): 04016202. doi.org/10.1061/(ASCE)ST.1943-541X.0001697

14. Doshi, Sagar M., and Thostenson, Erik T. "Novel Carbon Nanotube-Based Non-Woven Composite Sensors: Processing, Characterization and Potential Applications." *Proceedings of the American Society for Composites: Thirty-First Technical Conference*. 2016. www.dpi-proceedings.com/index.php/asc31/article/view/3183

15. Doshi Sagar M. and Thostenson Erik T. "Self-sensing carbon nanotube composites: processing and characterization" ed K Friedrich and U Breuer Multifunctionality of Polymer Composites (Amsterdam: Elsevier). 2015. doi.org/10.1016/C2013-0-13006-1

16. Hu, C. H., et al. "Resistance-pressure sensitivity and a mechanism study of multiwall carbon nanotube networks/poly (dimethylsiloxane) composites." *Applied Physics Letters* 93.3 (2008): 033108. doi.org/10.1063/1.2961028

17. An, Qi, Andrew N. Rider, and Erik T. Thostenson. "Hierarchical composite structures prepared by electrophoretic deposition of carbon nanotubes onto glass fibers." *ACS applied materials & interfaces* 5.6 (2013): 2022-2032. 10.1021/am3028734

18. Doshi, Sagar M., and Erik T. Thostenson. "Thin and Flexible Carbon Nanotube-Based Pressure Sensors with Ultrawide Sensing Range." *ACS sensors* 3.7 (2018): 1276-1282. 10.1021/acssensors.8b00378

19. An, Qi, Andrew N. Rider, and Erik T. Thostenson. "Electrophoretic deposition of carbon nanotubes onto carbon-fiber fabric for production of carbon/epoxy composites with improved mechanical properties." *Carbon* 50.11 (2012): 4130-4143. doi.org/10.1016/j.carbon.2012.04.061